

Z427/1033 (2009)- (17)



NUAA2010055215

Z427
1033 (2009) - (17)

自动化学院

032



2010055215

(17)

第4本

序号	作者姓名	职称	单位	论文题目	刊物名称	年卷期	提交人
107	姚志垒 肖嵐 严仰光 龚春英 吴婷 肖嵐 姚志垒	博士 生 教授 教授 教授 博士 生 教授	32	Push-pull forward three-level converter with reduced rectifier voltage stress	IEEE Applied Power Electronics Conference, 美国	2009. 1	肖嵐
108	肖嵐 姚志垒	教授 博士 生	32	双降压式全桥逆变器	中国电机工程学报	第29卷第15期, 2009	肖嵐
109	肖嵐 陈新	教授 副教授	32	研究生课程教学实践环节建设的思考	电气电子教学学报	第31卷第1期, 2009	肖嵐
110	曹海港 朱德明 肖嵐	硕士 生 博士 教授	32	电流反馈对步进电动机运行性能的影响	电力电子技术	第43卷第1期, 2009	肖嵐
111	徐蓉 肖嵐	硕士 生 教授	32	固定关断时间PFC在CCFL中应用的研究	电力电子技术	第43卷第3期, 2009	肖嵐
112	姚志垒 肖嵐 严仰光	博士 生 教授 教授	32	Dual-Buck Full-Bridge Inverter With Hysteresis Current Control	IEEE Transactions on Industrial Electronics	第56卷第8期, 2009年	肖嵐
113	姚志垒 肖嵐 严仰光	博士 生 教授 教授	32	Control Strategy for Series and Parallel Output Dual-Buck Half Bridge Inverters Based on DSP Control	IEEE Transactions on Power Electronics	2009, 24 (2)	肖嵐
114	王勤 王成华 郁斌 赵国安 戴文雯 肖嵐	副教授 授讲 师讲 师助 助教 教授	0320 3203 2032 0320 32	加强实验教学示范中心建设 培养高质量创新型人才	实验室研究与探索	第28卷12期, 第87-90页, 2009年12月	王勤
115	王勤 阮新波 韩璐	副高 正高 硕士	32	具有最大功率点跟踪功能的双输入反激DC/DC变换器	南京航空航天大学学报	第41卷6期, 第734-741页, 2009年12月	王勤
116	王勤 姚志垒 黄勇 肖嵐 阮新波	博士 生 硕 士 教 授	32	推挽正激三电平直流变换器及其控制策略	中国电机工程学报	第29卷第30期, 第13-19页, 2009年12月	王勤
117	庄凯 阮新波	博士 正高	032 032	输入串联输出并联逆变器的均压稳定性分析	中国电机工程学报	2009, 24 (4)	阮新波
118	庄凯 阮新波	博士 正高	032 032	输入串联输出并联逆变器的分布式均压控制策略	电工技术学报	2009, 24 (5)	阮新波

119	庄凯 阮新波 张友军 阮新波 陈澄 陈志娟 张欣 Henry-S.H.Chung 阮新波 A.Ioionovic	博士 正高 博士 正高 学士 学士 博士 正高	032 032 032 032 032 032 032 032	输入串联输出并联逆变器的集中式均压控制策略 励磁电流实现不对称半桥直流变换器ZVS的研究 A ZCS Full-Bridge Converter without Voltage Over-Stress on the Switches Small Signal model for Boost Phase-shifted Full Bridge converter in High Voltage application A Novel ZVS PWM Phase-shifted Full-bridge Converter with Controlled Auxiliary Circuit Boost-Flyback Single-Stage PFC Converter with Large DC Bus Voltage Boost-Flyback 单级PFC变换器 Designing of Coupled Inductor in Interleaved Critical Conduction Mode Boost PFC Converter Multiple-input Full Bridge DC-DC Converter 超声电机的软开关驱动电路 旋转型行波超声电机的等效电路模型 The Input Voltage Sharing Control Strategy for Input-Series and Output-Parallel Converter under Extreme Conditions 极端条件下输入串联输出并联直流变换器均压控制策略 高压大功率场合LLC谐振变换器的分析与设计	电工技术学报 电力电子技术 IEEE Energy Conversion Congress and Exposition IEEE Energy Conversion Congress and Exposition IEEE Applied Power Electronics Conference and Exposition IEEE Energy Conversion Congress and Exposition 南京航空航天大学报 IEEE Energy Conversion Congress and Exposition IEEE Energy Conversion Congress and Exposition 中国电机工程学报 中国电机工程学报 IEEE Energy Conversion Congress and Exposition 电工技术学报 电工技术学报	2009, 24 (4) 2009, 24 (6) 2009 2009 2009 2009, 41(4) 2009 2009, 29 (3) 2009, 29 (15) 2009 2009, 24 (12) 2009, 24 (5)	阮新波 阮新波 阮新波 阮新波 阮新波 阮新波 阮新波 阮新波 阮新波 阮新波 阮新波 阮新波 阮新波 阮新波 阮新波
120							
121							
122							
123							
124							
125							
126							
127							
128							
129							
130							
131							
132							

133	王学华 阮新波 王蓓蓓 张欣	博士 正高 硕士 博士	032 032 032 032	阶梯波合成II型混合级联多电平逆变器的功率均衡策略	电工技术学报	2009, 24 (2)	阮新波
134	王学华 张欣 阮新波 阮新波 陈武 程璐璐 Chi K.Tse 颜红 章涛 任小永 阮新波 钱海 李明秋 陈乾宏 任小永 阮新波 钱海 李明秋 陈乾宏	博士 博士 正高 正高 正高 博士 硕士 硕士 博士 博士 正高 正高 硕士 硕士 正高 博士 正高 正高	032 032 032 032 032 032 032 032 031 031 031 031 032 032 032 032 032	SPWM控制策略及其功率均衡方法	电工技术学报	2009, 24 (5)	阮新波
135	Control Strategy for Input-Series-Output-Parallel Converters	IEEE Transactions on Industrial and Electronics	2009, 56 (4)	阮新波			
136	Three-Mode Dual-Frequency Two-Edge Modulation Scheme for Four-Switch Buck-Boost Converter	IEEE Transactions on Power Electronics	2009, 24 (2)	阮新波			
137	双沿调制的四开关Buck-Boost变换器	中国电机工程学报	2009, 29 (12)	阮新波			
138	A Novel Power Management Control Strategy for Stand-alone Photovoltaic Power System	the 6th International Power Electronics and Motion Control Conferencetion	2009	阮新波			
139	任意光强和温度下的硅太阳电池非线性工程简化数学模型	太阳能学报	2009, 30 (4)	阮新波			
140	带缓冲单元的多输入直流变换器电路拓扑	电工技术学报	2009, 24 (6)	阮新波			
141	无缓冲单元的多输入直流变换器电路拓扑	电工技术学报	2009, 24 (5)	阮新波			
142	双输入Buck变换器的交错双沿调制方法	电工技术学报	2009, 24 (4)	阮新波			
143	Modeling, Analysis and Design for Hybrid Power Systems with Dual-Input DC-DC Converter	IEEE Energy Coversion Congress and Exposition	2009	阮新波			
144	Effect of Duty Cycle on Common Mode Conducted Noise of DC-DC Converters	IEEE Energy Coversion Congress and Exposition	2009	阮新波			

145	顾琳琳 阮新波 徐明 姚凯	硕 士 正高 博士	032 032 032	Means of Eliminating Electrolytic Capacitor in AC/DC Power Supplies for LED Lightings	IEEE Transactions on Power Electronics	2009, 24 (5)	阮新波
146	陈武 庄凯 阮新波	博士 博士 正高	032 032 032	A Input-Series- and Output- Parallel-Connected Inverter System for High-Input- Voltage Applications	IEEE Transactions on Power Electronics	2009, 24 (9)	阮新波
147	陈武 阮新波 颜红 Chi K.Tse	博士 博士 正高 硕士 K.Tse	032 032 032 032	DC/DC Conversion Systems Consisting of Multiple Converter Modules: Stability, Control, and Experimental Verification	IEEE Transactions on Power Electronics	2009, 24 (6)	阮新波
148	陈武 阮新波 颜红 陈武	博士 正高 硕士 博士	032 032 032 032	多变换器模块化串并联组 合系统	电工技术学报	2009, 24 (6)	阮新波
149	阮新波 颜红	正高 硕士	032 032	DC/DC多模块串并联组合 系统控制策略	电工技术学报	2009, 4 (7)	阮新波
150	陈武 阮新波 庄凯	博士 正高 博士	032 032 032	Input-Series and Output- Parallel Connected Inverter System for High Input Voltage Applications	IEEE Applied Power Electronics Conference and Exposition	2009	阮新波
151	李秀娟 陈明恩	副高 硕士	035 035	应用蓝牙技术的多通道数 据采集与传输系统	哈尔滨工业大学学 报	2009, 41 (5)	李秀娟
152	陈乾宏	正高	032	Gyrator-Capacitor Simulation Model of Nonlinear Magnetic Core	APEC 2009-Twenty- Fourth Annual IEEE Applied Power Electronics Conference and Exposition	1740-1746	陈乾宏
153	陈乾宏	正高	032	Analysis, Design, and Control of a Transcutaneous Power Regulator for Artificial Hearts	IEEE TRANSACTIONS ON BIOMEDICAL CIRCUITS AND SYSTEMS	VOL. 3, NO. 1, FEB RUARY 2009	陈乾宏
154	陈乾宏 冯阳 周林泉 王健 阮新波	正高 硕士 硕士 硕士 正高	0320 3203 2032 032	输出文博最小化有源箝位 正激磁集成变换器	中国电机工程学报	第23卷第3期, 第 7-13页, 2009年1 月	陈乾宏
155	陈乾宏 李竹筠 徐立刚 陈乾宏 徐立刚 李竹筠 任小永 阮新波 徐立刚 陈乾宏 朱祥 丰骏	正高 硕士 正高 硕士 正高 硕士 博士 正高 硕士 正高 硕士 正高	032 0320 3203 2032 032 032 3203 2032 032 0320 3203 2032	回转器-电容模型的教学研 究	电气电子教学学报	第31卷第1期, 2009	陈乾宏
156				改进型回转器-电容非线性 磁心仿真模型	电工技术学报	第24卷第4期, 第 14-21页, 2009年 4月	陈乾宏
157				单相整流滤波电容纹波电 流的数学模型与分析	电力电子技术	第43卷第3期, 2009	陈乾宏

173	穆建国 王莉 胡杰	硕士 正高 硕士	032 032 032	Analysis and Design of Topological Structure for DC Solid-State Circuit Breaker Design of DC Architecture for Large-Scale Non-Grid-Connected Wind Power Generation System	2009 World Non-Grid-Connected Wind Power and Energy Conference APPEEC 2009	2009, P312-316	王莉
174	陈杰 张先进 陈冉 龚春英	博士 博士 博士 教授	032 032 032 032	Decoupling Control of the Non-Grid-Connected Wind Power System with the Droop Strategy Based on a DC Micro-Grid Design of the DC/DC Converter for Aerodynamic Characteristics Testing of Wind Turbine	WNWEC 2009	2009	龚春英
175	陈杰 陈家伟 陈冉 龚春英	博士 博士 博士 教授	032 032 032 032	Decoupling Control of the Non-Grid-Connected Wind Power System with the Droop Strategy Based on a DC Micro-Grid Design of the DC/DC Converter for Aerodynamic Characteristics Testing of Wind Turbine	WNWEC 2009	2009	龚春英
176	陈家伟 陈杰 张先进 龚春英	博士 博士 博士 教授	032 032 032 032	A new voltage control method for DC grid in distributed generationa A Novel Dual Boost/Dual Buck AC/AC Converter	6th International Power Electronics and Motion Control Conference 6th International Power Electronics and Motion Control Conference	2009	龚春英
177	张先进 陈杰 龚春英	博士 博士 教授	032 032 032	A new voltage control method for DC grid in distributed generationa A Novel Dual Boost/Dual Buck AC/AC Converter	6th International Power Electronics and Motion Control Conference 6th International Power Electronics and Motion Control Conference	2009	龚春英
178	陈家伟 陈杰 龚春英	博士 博士 教授	032 032 032	LLC半桥谐振变换器参数设计法的比较与优化 反激式平面变压器绕组交流损耗的分析 高压输入低压大电流输出模块电源的设计	电力电子技术 电力电子技术 电力电子技术	2009 年43 卷 11期 2009年43卷3期 2009年43 卷 5期	龚春英 龚春英 龚春英
179	江雪 龚春英	硕士 教授	032 032	LLC半桥谐振变换器参数设计法的比较与优化	电力电子技术	2009 年43 卷 11期	龚春英
180	丁秀华 祝锦 龚春英	硕士 硕士 教授	032 032 032	反激式平面变压器绕组交流损耗的分析	电力电子技术	2009年43卷3期	龚春英
181	丁秀华 邓翔 龚春英	硕士 讲师 教授	032 032 032	高压输入低压大电流输出模块电源的设计	电力电子技术	2009年43 卷 5期	龚春英
182	陈杰 张先进 龚春英	博士 博士 教授	032 032 032	基于直流电网的非并网风电系统及其控制策略	电力系统自动化	2009年33卷10期	龚春英
183	刘大刚 陈杰 龚春英	硕士 博士 教授	032 032 032	双Buck逆变器的磁集成技术研究	电力电子技术	2009年 43卷3期	龚春英
184	朱铭炼 于正友 孙娇俊	硕士 硕士 硕士	032 032 032	一种新颖的主动移频式孤岛检测方法	电力电子技术	2009年43卷11 期	龚春英
185	孙涛 龚春英	硕士 教授	032 032	一种用于燃料电池发电系统的前级DC/DC变换器	电力电子技术	2009年43卷 2 期	龚春英

186	刘磊 王建华 龚春英	硕士 博士 教授	032 032 032	一种组合式三相逆变器基 准信号的产生方法	电力电子技术	2009年43卷1期	龚春英
187	张先进 陈杰 龚春英	博士 博士 教授	0320 3203 2	直流变压器研究	高电压技术	2009年35卷5期	龚春英
188	金科 阮新波 杨孟雄 徐敏	正高 正高 硕士 硕士	032 032 032 032	Power management for fuel cell power system cold start	IEEE Transactions on Power Electronics	2009, 24(10)	金科
189	金科 阮新波 杨孟雄 徐敏	正高 正高 硕士 硕士	032 032 032 032	A hybrid fuel cell power system	IEEE Transactions on Industrial Electronics	2009, 56(4)	金科
190	金科 Ming Xu F.C. Lee Yi Sun	正高	032	Self-driven schemes for a 12V self-driven voltage regulator	IEEE Energy Conversion Congress and Exposition	2009	金科
191	金科 Ming Xu Yi Sun Doug Sterk F.C. Lee	正高	032	Evaluation of self-driven schemes for 12V self-driven voltage regulator	IEEE Transactions on Power Electronics	2009, 24(10)	金科
192	张卓然 严仰光 杨善水 周波	副高 正高 副高 正高	032 032 0320 32	Development of a new permanent magnet BLDC generator using 12-phase half-wave rectifier	IEEE Transaction on Industrial Electronics	2009, 56(6)	张卓然
193	张卓然 严仰光	副高 正高	032 032	Influence of Winding Inductance on Output Characteristic of Low Speed Doubly Salient Wind Power Generator	Proceedings of The 12th International Conference on Electrical Machines and Systems(ICEMS) 2009	Nov. 2009.	张卓然
194	Zhuora n Zhang, Yangg uang Yan, Zhang Quan, Tao Yangya ng, and Zhou Bo	副高 正高 硕士 硕士 正高	032 032 0320 32 032	Development of A New Low Speed 24-32-poles Doubly Salient Wind Turbine Generator	World Non-grid- connected Wind Power and Energy Conference	Sept.2009	张卓然

206	张之梁 Jizhen Fu, 副高 Yan- 硕士 Fei 正高 Liu, 正高 Paresh Sen	032	A new discontinuous current-source driver for high frequency power MOSFETs	IEEE Energy Conversion Congress and Exposition (ECCE), 2009	2009 年 1655-1662页	张之梁
207	张之梁 Eric Myer, Yan- 副高 Fei 博士 Liu, 正高 Paresh Sen	032	A new ZVS non-isolated full-bridge VRM with synchronous rectifier gate energy recovery	IEEE Applied Power Electronics Conference (APEC), 2009	2009 年 1469-1475页	张之梁
208	张之梁 Wilson Eberle 副 , 高 Yan- 讲师 Fei 正高 Liu, 正高 Paresh Sen	032	A novel non-isolated ZVS asymmetrical buck voltage regulator module with direct energy transfer	IEEE Transaction on Industrial Electronics.	Vol. 56, No. 8, Aug. 2009, pp. 3096-3105	张之梁
209	陈新 硕士 马海啸 副高 龚春英 正高	032	应用于航空变频电源系统的新型串联混合有源滤波器	航空学报	2009, 12 (30)	陈新
210	马运东 副高 胡祖荣 硕士 王俊琦 硕士 赖日新 硕士 邢岩 正高	032	Research on fixed-pitch wind turbine running in deep stall regime	2009第一届世界非并网风能与能源大会论文集	2009	马运东
211	胡祖荣 硕士 王俊琦 硕士 马运东 副高 邢岩 正高	032	Research on speed control system for fixed-pitch wind turbine based on disturbance observer	2009第一届世界非并网风能与能源大会论文集	2009	马运东
212	王俊琦 硕士 马运东 副高 胡祖荣 硕士 邢岩 正高	032	Modeling and real-time simulation of non-grid-connected wind energy conversion system	2009第一届世界非并网风能与能源大会论文集	2009	马运东
213	胡祖荣 硕士 马运东 副高 王俊琦 硕士 邢岩 正高	032	基于扰动观测器的定桨距风力机转速控制研究	中国电源学会第十八届学术年会论文集	2009	马运东
214	马运东 副高 王芳 中级	032	电气工程教学中提高仿真教学效果的方法研究	第6届全国高等学校电气工程及其自动化专业教学改革研讨论文集	2009	马运东

215	SHI WEI 邢岩 马运东 赖日新	0320 3203 2032	Modeling and Control for a Non-Grid- Connected Wind Power System Based on a Fixed-Pitch Variable Speed Wind Turbine and a Doubly Salient Generator Three-level Reversible Converter for Large- scale Non-Grid- Connected Wind Power System	WNWEC 2009	邢岩
216	王充 邢岩 fangyu 马运东		Optimum Feed-Forward Control for UPFC Converters in Large- scale Non-Grid- Connected Wind Power Applications	WNWEC 2009	邢岩
217	倪晶朦 nongsu n		A single-state Forward Inverter with High Frequency Isolation for Grid-connected Application	WNWEC 2009	邢岩
218	张力 冯兰 兰邢 岩 马运 东 华明		Decoupled Control of Inverters in Parallel Operation for AC Motor Drives	IECON 2009	邢岩
219	胡海兵 邢岩 何中翼	博士 032	An Ultra-capacitor Based Regenerating Energy Storage System for Urban Rail Transit	IECON 2009	
220	许爱国 谢少军 姚远 刘小宝 冯晶晶	教授 032 硕士 032 硕士 032 硕士 032	Dynamic Voltage Equalization for Series-Connected Ultracapacitors in EV/HEV Applications	IEEE ECCE 2009	2009 谢少军
221	许爱国 谢少军 刘小宝	博士 032 教授 032 硕士 032	Research on Voltage Equalization of Serial Ultracapacitors	IEEE Trans. on VT	2009, 58, 8 谢少军
222	许爱国 刘小宝 谢少军	博士 032 硕士 032 教授 032	Study on Dual-Loop Grid Current Control Scheme for Grid- Connected Inverter with an LCL-Filter A Multipulse- Structure-Based Bidirectional PWM Converter for High- Power Applications	IEEE ICIEA 2009	2009 谢少军
223	许爱国 徐志英 谢少军	博士 032 硕士 032 教授 032		IEEE ICIEA 2009	2009 谢少军
224	许爱国 谢少军	博士 032 教授 032		IEEE Trans. on PE	2009, 24, 5 谢少军

225	许爱国 谢少军	博士 教授	032 032	A Multi-Pulse Structure Based AC-DC/DC-AC PWM Converter for High Power Application	IEEE APEC 2009	2009	谢少军
225	许爱国 刘小宝 谢少军	博士 硕士 教授	032 032 032	Research on dynamic voltage equalization circuit for series connected ultracapacitors	IEEE ICIT 2009	2009	谢少军
226	许爱国 谢少军	博士 教授	032 032	A Novel Waveform Modulation Method for Staircase Inverters	IEEE ICIT 2009	2009	谢少军
227	汤雨 谢少军 张超华	博士 教授 硕士	032 032 032	Feedforward Plus Feedback Control of the Improved Z-source Inverter	IEEE ECCE 2009	2009	谢少军
228	汤雨 谢少军 张超华 许泽刚	博士 教授 硕士 博士	032 032 032 032	Improved Z-Source Inverter With Reduced Z-Source Capacitor Voltage Stress and Soft-Start Capability	IEEE Trans. on PE	2009, 24, 2	谢少军
229	汤雨 张超华 谢少军	博士 硕士 教授	032 032 032	New Structure and Topological Derivation of Z-Source Converters	IEEE ICIEA2009	2009	谢少军
230	刘海春 徐立智 谢少军	讲师 硕士 正高	032 032 032	A New Detection Method of Voltage Sag Based on Period Phase Concept	IEEE ICIEA2009	2009	刘海春
231	刘海春 丁志辉 谢少军	讲师 硕士 正高	032 032 032	A Novel Hybrid Current Control Strategy Applied in Three-Phase Four-Leg APF	IEEE IPEMC2009	2009	刘海春
232	刘海春 徐立智 谢少军	讲师 硕士 正高	032 032 032	A Method For Detecting Fundamental Current Based on 2nd Order Series Resonant Filter	IEEE IPEMC2009	2009	刘海春
233	毛鹏 谢少军	博士 教授	032 032	Current Phase Lag Issue and the Compensation Scheme for OCC PFC Converter	IEEE IPEMC 2009	2009	谢少军
234	徐志英 许爱国 谢少军	硕士 博士 教授	032 032 032	采用LCL滤波器的并网逆变器双闭环入网电流控制技术研究	中国电机工程学报	2009, 29, 27	谢少军
234	谢少军 汤雨 张超华	教授 博士 硕士	032 032 032	Research on third harmonic injection control strategy of improved Z-Source inverter	IEEE ECCE 2009	2009	谢少军
235	许爱国 谢少军	博士 教授	032 032	阶梯波合成逆变器的波形调制技术研究	中国电机工程学报	2009, 29, 21	谢少军

Push-Pull Forward Three-Level Converter with Reduced Rectifier Voltage Stress

Zhilei Yao^{1,2}, Lan Xiao¹, Yong Huang¹, and Chunying Gong¹

¹Nanjing University of Aeronautics and Astronautics, Nanjing 210016, P.R. China;

²Yancheng Institute of Technology, Yancheng 224051, P.R. China

Abstract-This paper proposes a push-pull forward (PPF) three-level (TL) converter, which is suitable for low and wide-range input voltage applications, such as fuel cell power system. Half of the switches sustain half of the input voltage, and the others sustain one and one-half input voltage. Input ripple current and output filter inductor ripple current can be reduced with the TL waveform of the secondary rectified voltage. However, voltage stress of the rectifier diode is high with the conventional TL control strategy in a high output-voltage situation, considering voltage spike across the rectifier diode caused by the leakage inductance. When 1/2 level of the secondary rectified voltage shows first, and 1 level of that appears later, the voltage stress of the rectifier diode can be reduced by paralleling with external capacitor. Operating principle, control strategy, and selection of the external capacitor are analyzed. Finally, experimental results verify the theoretical analysis.

I. INTRODUCTION

Available fossil fuel reserves and environment concern are now the driving source to the use of new clean and renewable energy sources [1], such as photovoltaic energy, wind energy and fuel cell. The emission of fuel cell is only water, and the noise is very low, so it has been receiving more and more attention in distributed generation power systems [2] and electrical vehicles [3]–[6]. Dc-dc converter is an important part of them [7]–[8].

As the output voltage of fuel cell is often low [9], the push-pull forward (PPF) converter has been attracted considerable attention on built-in input filter and voltage-spike reduction of the main switches by the clamping capacitor [10]–[13].

However, the output voltage of fuel cell fluctuates with the load [9], such as 50 V – 90 V, so the input ripple current should be low. The three-level (TL) converter has been proposed to reduce the voltage stresses of the switches, input filter and output filter [14]–[15]. However, the conventional TL converter often presents 1 level of the secondary rectified voltage first, so the voltage stress across the rectifier diode is high [16]–[17], especially under high output-voltage condition. For example, when the dc-dc converter is as the front stage of a full-bridge inverter that provides the voltage of 220 Vac, the output voltage of the dc-dc converter should be about 360 V, and the voltage stress of rectifier diode is

about 700 V. Therefore, it is difficult to select the rectifier diode considering the voltage spike caused by leakage inductance of the transformer and the reverse recovery of the rectifier diode.

In order to reduce the voltage oscillation across the rectifier diode, two clamping diodes are introduced to the primary side [17]–[20]. However, it can only eliminate the voltage spike across the rectifier diode caused by the resonant inductor, and it still cannot get rid of the voltage spike caused by the leakage inductance of the transformer, which cannot be ignored, especially in a high output-voltage situation, as the reverse recovery of the rectifier diode cannot be neglected [21].

Another method is to add a secondary passive snubber [22]. The voltage spike across the rectifier diode can be reduced by the appropriate selection of the snubber capacitors, but the minimum value and maximum value of the duty cycle are affected by the snubber capacitors, and thus the output voltage is influenced, e.g., the output voltage may generate a overshoot voltage at slight load under high input voltage condition.

In order to solve the aforementioned problems, this paper proposes a PPF TL converter. It integrates the advantages of the PPF and the TL converters. Half of the switches sustain half of the input voltage, and the others sustain one and a half of the input voltage. The voltage stress of the rectifier diode can be reduced by the control strategy and external paralleled capacitor. Operating principle of the proposed converter is illustrated in Section II, whereas the control strategy is described in Section III. Selection of the external capacitor is analyzed in Section IV. Finally, Experimental results from a 500 W PPF TL converter confirm the theoretical analysis in Section V.

II. OPERATING PRINCIPLE

Fig. 1 shows the main circuit of the proposed converter, where $S_1 \sim S_4$ are the main power switches, $C_{s1} \sim C_{s4}$ are the output capacitors of $S_1 \sim S_4$, $D_{s1} \sim D_{s4}$ are the body diodes of $S_1 \sim S_4$, and D_5 and D_6 are the clamping diodes.

The switches S_1 and S_4 are PWM controlled, and S_2 and S_3 are switched 180° out of phase with a small dead time. As the total charge Q_g of low voltage-stress MOSFET is often lower than that of high one [21], S_1 and S_4 are turned off very little earlier than S_2 and S_3 , respectively. The drain-source voltage of S_1 and S_4 can be clamped to half of the input voltage by

This work was supported in part by Support Fund of Aviation Science and Technology under Award 05C52006, Fund of Colleges Production Industrialization in Jiangsu Province under Award 051a150018, and Fund of Science and Technology Production Transformation in Jiangsu Province.

D_5 and D_6 , respectively, and the drain-source voltage across S_2 and S_3 can be clamped to one and a half of the input voltage by the flying capacitor (C_{ss}) and the clamping capacitor (C). The switches S_2 and S_3 are the leading switches, and S_1 and S_4 are the lagging switches, so the 1/2 level of the secondary rectified voltage appears first.

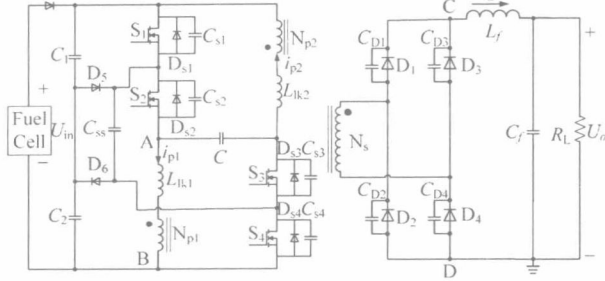


Fig. 1. Main circuit of the PPF TL converter.

Before the analysis, we make the following assumptions:

- 1) all the diodes are ideal, except for the rectifier diodes $D_1 \sim D_4$, which are equivalent to ideal diodes and paralleled capacitors to simulate the reverse recovery, junction capacitances, and external paralleled capacitors;
- 2) all the inductors, capacitors and transformer are ideal, except for the leakage inductances L_{lk1} and L_{lk2} of the transformer, and $L_{lk1} = L_{lk2} = L_{lk}$;
- 3) $C_{s1} = C_{s4} = C_{lag}$, $C_{s2} = C_{s3} = C_{lead}$, $C_{D1} = C_{D2} = C_{D3} = C_{D4} = C_D$;
- 4) the divided capacitors C_1 and C_2 are equal and large enough to be treated as two voltage sources with a value of $U_{in}/2$;
- 5) C is large enough, and its voltage in steady state equals to input voltage (U_{in}); and
- 6) C_{ss} is large enough, and its voltage in steady state is $U_{in}/2$.

Fig. 2 shows the key waveforms of the proposed converter, where $u_{ds1} \sim u_{ds4}$ are the drain-source voltage of $S_1 \sim S_4$, respectively. There are 20 switching modes in a switching period, and a set of corresponding equivalent circuits is given in Fig. 3 to aid in understanding each mode.

1) Mode 1 [before t_1] [Refer to Fig. 3(a)]: Circuit is in steady state. S_1 , S_2 , D_1 , and D_4 are conducting, and the primary side powers the load.

2) Mode 2 [t_1, t_2] [Refer to Fig. 3(b)]: At t_1 , S_1 is turned off. The further simplified equivalent circuit of mode 2 is given in Fig. 4(a), where C_D' is the equivalent capacitor of C_D to the primary, and I_o' is the reflected filter inductor current at t_1 , which can be considered as a current source at the small interval. C_{s1} , C_{s4} , C_D' , and L_{lk} begin to resonate, making u_{ds1} increase from zero and u_{ds4} fall from $U_{in}/2$. The filter inductor current is divided into two parts: one part is reflected to the primary to charge C_{s1} and discharge C_{s4} via C_{ss} ; the other part discharges C_{D2} and C_{D3} .

$$u_{ds4}(t) = U_{in}/2 - u_{ds1}(t) \quad (1)$$

$$u_{ds1}(t) = \frac{C_D' I_o'}{2C_{lag}(C_D' + C_{lag})\omega_1} \sin \omega_1(t - t_1) + \frac{I_o'}{2(C_D' + C_{lag})} (t - t_1) \quad (2)$$

$$u_{C_D'}(t) = U_{in} + \frac{I_o'}{2(C_D' + C_{lag})\omega_1} \sin \omega_1(t - t_1) - \frac{I_o'}{2(C_D' + C_{lag})} (t - t_1) \quad (3)$$

$$i_p(t) = \frac{C_D' I_o'}{C_D' + C_{lag}} \cos \omega_1(t - t_1) + \frac{C_{lag} I_o'}{C_D' + C_{lag}} \quad (4)$$

where $\omega_1 = \sqrt{(C_D' + C_{lag})/C_D' L_{lk} C_{lag}}$ and $i_p = i_{p1} + i_{p2}$.

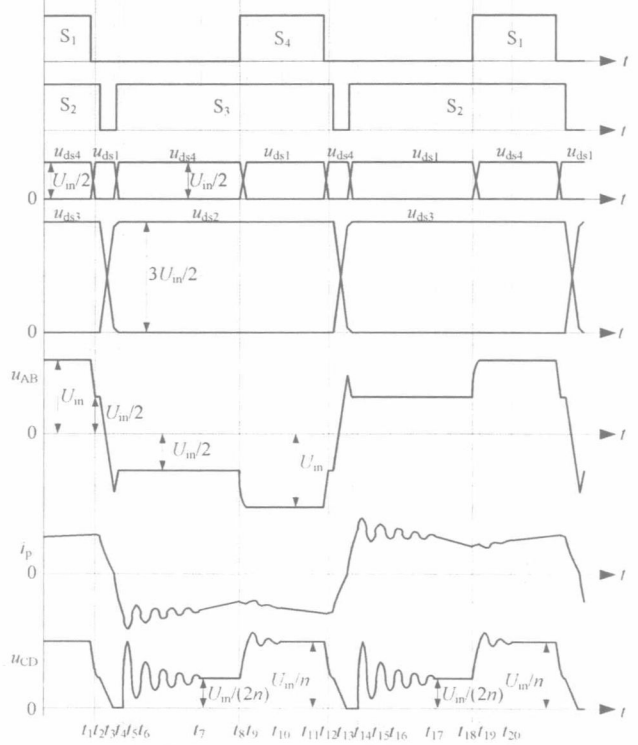


Fig. 2. Key waveforms of the PPF TL converter.

3) Mode 3 [t_2, t_3] [Refer to Fig. 3(c)]: At t_2 , D_{s4} and D_5 are conducting, so the transformer primary voltage, u_{AB} , is equal to $U_{in}/2$. The current i_p decays. Fig. 4(b) shows the further simplified equivalent circuit of mode 3. C_D' and L_{lk} start to resonate, and C_{D2} and C_{D3} are discharging.

$$u_{C_D'}(t) = \frac{U_{in}}{2} + \frac{(I_1 - I_o')}{2C_D' \omega_2} \sin \omega_2(t - t_2) - \frac{U_{in} - 2U_{C_D'}(t_2)}{2} \cos \omega_2(t - t_2) \quad (5)$$

$$i_p(t) = (I_1 - I_o') \cos \omega_2(t - t_2) + \frac{U_{in} - 2U_{C_D'}(t_2)}{L_{lk} \omega_2} \sin \omega_2(t - t_2) + I_o' \quad (6)$$

where $\omega_2 = \sqrt{1/(C_D' L_{lk})}$, and I_1 is the value of i_p at t_2 .

4) Mode 4 [t_3, t_4] [Refer to Fig. 3(d)]: At t_3 , S_2 is gated off. The further simplified equivalent circuit of mode 4 is shown in Fig. 4(c). C_{s2} , C_{s3} , C_D' , and L_{lk} commence to resonate, so as to u_{ds2} increases from zero and u_{ds3} falls from $3U_{in}/2$. C_{D2} and C_{D3} continue to discharge, and i_p declines.

$$u_{ds2}(t) = \frac{C_D' I_2}{2C_{lead}(C_D' + C_{lead})\omega_3} \sin \omega_3(t - t_3) + \frac{I_2}{2(C_D' + C_{lead})}(t - t_3) \quad (7)$$

$$u_{ds3}(t) = 3U_{in}/2 - u_{ds2}(t) \quad (8)$$

$$i_p(t) = \frac{C_D' I_2}{C_D' + C_{lead}} \cos \omega_3(t - t_3) + \frac{C_{lead} I_2}{C_D' + C_{lead}} \quad (9)$$

$$u_{C_D'}(t) = U_{C_D'}(t_3) + \frac{I_2}{2(C_D' + C_{lead})\omega_3} \sin \omega_3(t - t_3) - \frac{I_2}{2(C_D' + C_{lead})}(t - t_3) \quad (10)$$

where $\omega_3 = \sqrt{(C_D' + C_{lead})/C_D' L_{lk} C_{lead}}$, and I_2 is the value of i_p at t_3 .

5) Mode 5 [t_4, t_5] [Refer to Fig. 3(e)]: At t_4 , D_2 and D_3 are forward biased, and all the four rectifier diodes conduct, which clamp both the transformer primary and secondary voltage at zero. Fig. 4(d) presents the further simplified equivalent circuit of mode 5. C_{s1} , C_{s4} , C_{s2} , and C_{s3} resonate with L_{lk} . The current i_p continues to decay.

$$u_{ds1}(t) = \frac{U_{in}}{2} \cos \omega_4(t - t_4) \quad (11)$$

$$u_{ds4}(t) = U_{in}/2 - u_{ds1}(t) \quad (12)$$

$$u_{ds3}(t) = U_{ds3}(t_4) \cos \omega_4(t - t_4) \quad (13)$$

$$u_{ds2}(t) = 3U_{in}/2 - u_{ds3}(t) \quad (14)$$

$$i_p(t) = I_3 - C_{lead} U_{in} \omega_4 \sin \omega_4(t - t_4) \quad (15)$$

where $\omega_4 = \sqrt{(C_{lead} + C_{lag})/L_{lk} C_{lead} C_{lag}}$, and I_3 is the value of i_p at t_4 .

During this mode, S_3 is gated on.

6) Mode 6 [t_5, t_6] [Refer to Fig. 3(f)]: At t_5 , u_{ds1} and u_{ds3} decrease to zero, u_{ds4} increases to $U_{in}/2$, and u_{ds2} reaches to $3U_{in}/2$. Therefore, $U_{in}/2$ is applied on L_{lk1} and L_{lk2} , which makes i_p decay linearly.

$$i_p(t) = I_4 - (U_{in}/L_{lk})(t - t_5) \quad (16)$$

where I_4 is the value of i_p at t_5 .

7) Mode 7 [t_6, t_7] [Refer to Fig. 3(g)]: At t_6 , i_p reaches to the reflected filter inductor current $-I_l(t_6)/n$, where n is the winding ratio of the primary and secondary windings of the transformer. Therefore, all the filter inductor current flows through C_{D2} and C_{D3} . The further simplified equivalent circuit of mode 7 is presented in Fig. 4(e). C_D' and L_{lk} initiate to resonate.

$$u_{C_D'}(t) = U_{in}/2 - (U_{in}/2) \cos \omega_5(t - t_6) \quad (17)$$

$$i_p(t) = -I_l(t_6)/n - C_D' \omega_5 U_{in} \sin \omega_5(t - t_6) \quad (18)$$

where $\omega_5 = \sqrt{1/(C_D' L_{lk})}$.

During this period, the voltage across C_{D1} and C_{D4} resonates between 0 and U_{in}/n , but damping exists in the practical system, e.g., the conduction resistance of the MOSFET, the winding resistance of the transformer. Thus, the voltage across C_{D1} and C_{D4} decay to $U_{in}/(2n)$ gradually. If the 1 level of the secondary rectified voltage appears first, the voltage across the rectifier diode is $2U_{in}/n$, which is twice of that compared with the proposed method.

8) Mode 8 [t_7, t_8] [Refer to Fig. 3(h)]: At t_7 , the voltage across C_{D1} and C_{D4} approximate to $U_{in}/(2n)$. The current i_p decays linearly.

$$i_p(t) = I_5 - \frac{U_{in}/2 - nU_o}{n^2 L_f}(t - t_7) \quad (19)$$

where I_5 is the value of i_p at t_7 .

9) Mode 9 [t_8, t_9] [Refer to Fig. 3(i)]: At t_8 , S_4 is gated on. The further simplified equivalent circuit of mode 9 is shown in Fig. 4(f), where I_1' is absolute value of the reflected filter inductor current at t_8 , which can be considered as a current source. C_{s1} , C_{s4} , C_D' , and L_{lk} resonate, causing u_{ds1} to increase from zero and u_{ds4} to fall from $U_{in}/2$.

$$u_{ds1}(t) = \frac{C_D' I_1'}{2C_{lag}(C_D' + C_{lag})\omega_6} \sin \omega_6(t - t_8) + \frac{I_1'}{2(C_D' + C_{lag})}(t - t_8) \quad (20)$$

$$u_{ds4}(t) = U_{in}/2 - u_{ds1}(t) \quad (21)$$

$$u_{C_D'}(t) = \frac{U_{in}}{2} - \frac{I_1'}{2(C_D' + C_{lag})\omega_6} \sin \omega_6(t - t_8) + \frac{I_1'}{2(C_D' + C_{lag})}(t - t_8) \quad (22)$$

$$i_p(t) = -\frac{C_D' I_1'}{C_D' + C_{lag}} \cos \omega_6(t - t_8) - \frac{C_{lag} I_1'}{C_D' + C_{lag}} \quad (23)$$

where $\omega_6 = \sqrt{(C_D' + C_{lag})/C_D' L_{lk} C_{lag}}$.

10) Mode 10 [t_9, t_{10}] [Refer to Fig. 3(j)]: At t_9 , the voltage across C_{s4} decays to zero. The further simplified equivalent circuit of mode 10 is given in Fig. 4(g). C_D' and L_{lk} begin to resonate.

$$u_{C_D'}(t) = U_{in} - [U_{in} - U_{C_D'}(t_9)] \cos \omega_7(t - t_9) + \frac{(I_6 + I_1')}{2C_D' \omega_7} \sin \omega_7(t - t_9) \quad (24)$$

$$i_p(t) = -I_1' + 2C_D' \omega_7 [U_{in} - U_{C_D'}(t_9)] \sin \omega_7(t - t_9) + (I_6 + I_1') \cos \omega_7(t - t_9) \quad (25)$$

where $\omega_7 = \sqrt{1/(C_D' L_{lk})}$. I_6 is the value of i_p at t_9 .

As can be seen from (20), the third part on the right side is very small which can be neglected, so t_9 can be calculated from (20).